Cold Region Hydrology in a Changing Climate (Proceedings of symposium H02 held during IUGG2011 in Melbourne, Australia, July 2011) (IAHS Publ. 346, 2011).

Man-made oasis change and its effects on the hydrological regime of the Aksu River basin

SUXIA LIU, CHUN ZHANG, SHOUHONG ZHANG & XINGGUO MO

Key Laboratory of Water Cycle & Related Land Surface Processes, Institute of Geographic Sciences and Natural Resources Research, Chinese Academy of Sciences, Beijing 100101, China

liusx@igsnrr.ac.cn

Abstract By carefully classifying the NDVI spatial information retrieved from MODIS 13 over the Aksu Basin (China) into seven categories based on fractional vegetation cover, with a careful division of the whole study region (WS) into man-made sub-region (MMS) and natural sub-region (NS), and with special consideration of the seasonal difference between summer and winter, a new index, called the man-made oasis index (MMOI), to describe the extent of man-made oasis (EMMO), is proposed. It is expressed as the linear weighted combination of the area ratio of each class from III to VI to the total area, with the higher the class number the higher the weight. The reason to choose classes from III to VI is that in winter they can be only found in MMS. MMOI in winter in MMS shows an increasing trend over the last 10 years, which matches well with the increase of EMMO found from the documented study. A transfer function between MMOI in winter in MMS and EMMO is then proposed to calculate EMMO based on MMOI. As paddy field was only found located in MMS, evapotranspiration over the paddy field (ET_p) simulated by the VIP distributed eco-hydrological dynamic model was chosen as the rate representative of water consumption by man-made oasis (WCMMO) per unit of EMMO. WCMMO is then calculated yearly based on the ET_p information multiplied with EMMO based on the index MMOI. The simulated results of yearly WCMMO are useful in exploring the effects of the oasis on the hydrological regime of the Aksu River.

Key words index; man-made oasis; VIP distributed eco-hydrological model; water consumption; the Aksu River, China

INTRODUCTION

The Aksu River Basin (Fig. 1(a)), with the headwater rivers Toxkan and Kumarik flowing into the Aksu River, is located in the arid area of northwest China, to the south side of west Tianshan Mountain and northwestern part of Tarim Basin. The basin's area is 5.9×10^4 km^2, extending from 75°35′ to 80°59′E and from 40°17′ to 42°27′N. It is a sensitive geographical zone with glaciers in the mountain headwaters, the oasis in the midstream, and the desert in the downstream with very low precipitation, high evapotranspiration and scarce water resources. With the development of the economy, the area of natural oasis, including natural grassland, natural forest, wetland, river and lake, is changing, generating some new land units. These are called man-made oasis and include cultivated land, man-made forest, man-made grassland, urban and reservoirs (Liu *et al*., 2008). With the increase of the area of man-made oasis, it exerts influence on the hydrology of the Aksu River. All man-made oasis units need water. Each year large amounts of water are withdrawn and diverted from the river to irrigate the crops, trees and grass. Generally, the higher the level of economic development, the larger the extent of man-made oasis (EMMO), and the more the water consumed by the man-made oasis (WCMMO).

As water flowing by the Aksu region is not just for the use of the Aksu's economy, but also for the downstream environment, it is necessary to determine the rational EMMO of the Aksu region. The higher the EMMO, the more serious stress the downstream environment will face. A rational point of EMMO for the Aksu region is important for the sustainable development for the whole region.

In order to determine this rational point of EMMO, it is important to explore the relationship between EMMO and WCMMO. However, this is not an easy task as the method to exactly estimate both EMMO and WCMMO is not fully developed. The EMMO can be estimated by remote sensing image (e.g. Liu *et al*., 2008). However, it is time consuming to determine the EMMO on a yearly basis, which is essential building the relationship between EMMO and WCMMO. Usually the WCMMO is roughly estimated by the irrigation quota. However, this single value is not enough to establish the relationship. Furthermore, it may be possible to obtain the WCMMO information from river runoff changes. However, as the basin is incurring climate change (Shi *et al.*, 2002; Zhang *et al.*, 2010), it is difficult at present to separate the runoff changes caused by climate change and man-made oasis.

This paper proposes a new index, called the man-made oasis index (MMOI) to calculate the EMMO, based on the NDVI data derived from the Modis13 data (MODIS/Terra Vegetation Indices 16-Day L3 Global 250m SIN Grid V005). Daily runoff data collected at the Sharikilank station in the Toxkan River, Xehera station in the Kumarik River, Xidaqiao and Aral stations in the Aksu River from 1964 to 2008 are used to analyse the hydrological trend. There were missing data of runoff at Xehera (1973, 1974, 1990–2007), Xidaqiao (1967–1971, 1990–2000, 2006) and Aral (1968–69, 1972–73, 1975–76, 1990–2000). A process-based eco-hydrological model (VIP) is used to estimate the WCMMO with the information of EMMO. Meteorological data from 1960 to 2009 at 10 weather stations, including pan evaporation, sunshine duration, precipitation, temperature, and wind speed are used to drive the VIP model. The basin-wide average precipitation and temperature data are obtained by using the reverse square interpolation by the VIP model. Finally, the yearly WCMMO is calculated.

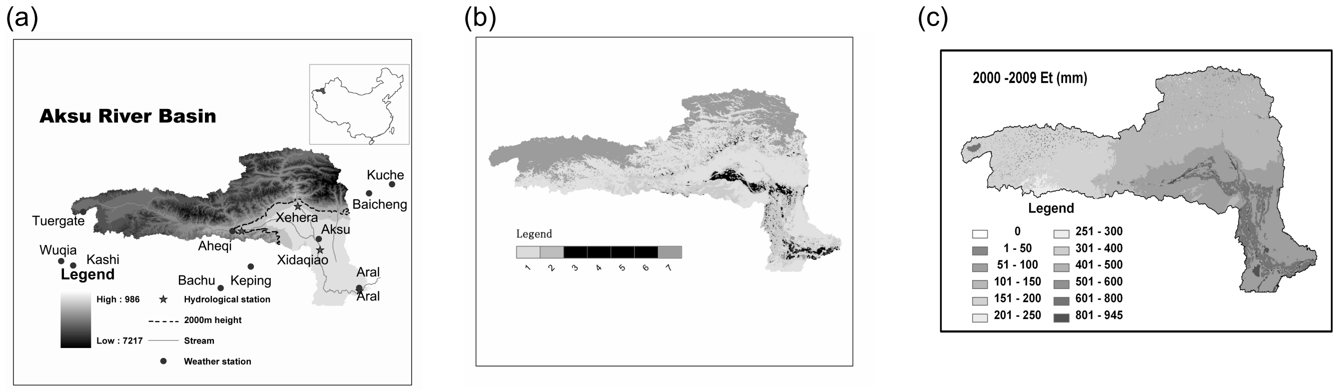

Fig. 1 (a) The Aksu River Basin, (b) distribution of classes III–VI (highlighted in black) in winter in 2009, and (c) the distribution of average evapotranspiration from 2000–2009 simulated by the VIP model.

METHOD

The Vegetation Interface Processes (VIP) model is used to simulate WCMMO. The VIP model (Mo *et al.*, 2009) was developed with the support of geographical information data. Its ecological and hydrological processes are coupled by a one-dimensional soil–vegetation–atmosphere transfer (SVAT) scheme, a distributed runoff routing scheme, and a vegetation dynamic scheme. The water cycle and energy transfer are coupled through evapotranspiration (ET, latent heat flux) process. Overland runoff is estimated with a variable infiltration curve, modified from Zhao (1992). Transfers of both overland and channel runoff are calculated with the kinematical wave equation. The estimation of canopy photosynthesis is based on Farquhar's biochemical model (Farquhar *et al.*, 1980). The canopy leaves are simplified into sunlit and shaded groups to account for their different photosynthesis responses to radiation, and a multilayer scheme is designed to describe the radiation penetration in canopy. Leaf area index (LAI) is the key state variable linking the hydrological processes and vegetation dynamics, which is derived from the foliage biomass.

Usually, after the ET over the grids is calculated based on the VIP model, annual WCMMO can be estimated for each year by summing up the values over those grids with man-made oasis recognized from the land-use map. However, this is not easy because the land-use map is only available for one limited period or at one single time point. Often we cannot obtain the yearly data of land-use cover. This encourages us to explore a new way to calculate yearly WCMMO.

Julian days 49 and 225 have been chosen to represent the typical conditions in the winter and summer seasons. NDVI distribution is obtained from the MODIS 13 for these two days for every year from 2000 to 2009. NDVI is then classified into seven categories shown in Table 1 according to the fractional vegetation cover (Chen, 2002):

$$F = (N - N_{min}) / (N_{max} - N_{min}) \tag{1}$$

where N is the value of NDVI multiplied by 10 000. Based on the vegetation information over the basin, we take N_{min} = 10 for winter, N_{min} = 56 for summer, and N_{max} = 9000 for both winter and summer.

Table 1 The definition of seven categories for the NDVI classification.

Fractional vegetation cover	0–10%	10–20%	20–40%	40–60%	60–80%	80–100%	Ice, snow and water
Class	I	II	III	IV	V	VI	VII

From the land use map obtained from the Environment Centre of Chinese Academy of Sciences (http://www.resdc.cn/first.asp) and the MODIS product, it is seen that most man-made oasis areas are located in areas of elevation below 2000 m (Fig. 1(a)). We thus divide the whole study region (WS) into two sub-regions, i.e. natural sub-region (NS) where elevation is above 2000 m, and man-made sub-region (MMS) where elevation is below 2000 m. Figure 2 shows the ratio of the area for each class to the total area for summer and winter averaged over the 10 years for WS, MMS, and NS. It is clear that in NS, classes from III to VI disappeared in winter, while in MMS they can be found. This is a strong indication that classes III to VI can be used to index human activity.

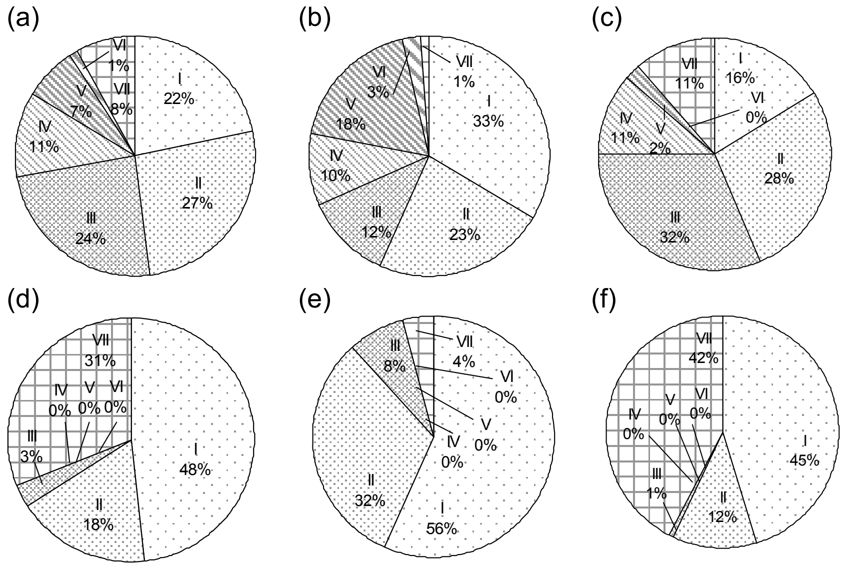

Fig. 2 The ratio of the area for each class to the total area for summer (upper panel) and winter (lower panel) averaged over the 10 years for WS (a), (d), MMS (b), (e) and NS (c), (f), respectively.

By comparing the distribution of classes III–VI in winter in the basin (Fig. 1(b)), it is clear that classes III–VI basically are distributed in the MMS area. It behaves like the footprint of the man-made oasis and can be used to index human activity. We thus propose the following index, called man-made oasis index (MMOI) to calculate EMMO:

$$O_q = 0.1 \times PLAND_{c3} + 0.2 \times PLAND_{c4} + 0.3 \times PLAND_{c5} + 0.4 \times PLAND_{c6} \tag{2}$$

where:

$$PLAND = Class\ area / Total\ area \times 100\% \tag{3}$$

c_3 to c_6 are classes III to VI, respectively. O_q is MMOI. The higher the class number, the higher the fractional vegetation cover. The larger the weight, the larger the EMMO. Based on MMOI plus the ET information from the VIP model, WCMMO can be obtained.

RESULTS

Figure 3(a) shows the annual precipitation record and its change over the Aksu River basin for the past 50 years. Precipitation slightly increased during 1955–2009, but significantly decreased in the last 10 years. Figure 3(b) shows the annual average temperature data and its change. There is a clear warming trend over the study period. In the last 10 years, temperature is rising with a relatively higher trend.

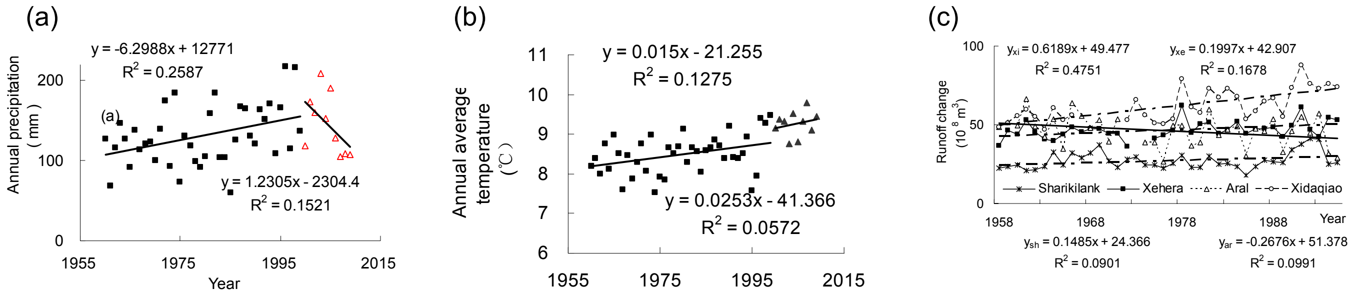

Fig. 3 (a) Precipitation data and change, (b) temperature data and change, and (c) annual runoff and changes, respectively, at the four hydrological stations.

Figure 3(c) shows the runoff data and changes during the past 51 years. Three hydrological stations, i.e. Sharikilank (Sh), Xidaqiao (Xi) and Xehera (Xe), have increasing trends, while the Aral station shows a weak decrease. The basin above the Xehera station receives a large supply of glacier melt water, as much as 52.4% (Wang, 2008). Runoff increase in this part of the basin may indicate snow and glacier melt water increases associated with temperature change (warming). On the other hand, the Aral (Ar) station, located at the downstream of the basin, shows a decreasing trend. This suggests that the effect of man-made oasis is larger than the effect of climate change, which counters its essential increasing trend with the increase of temperature. Studies (Shi *et al.*, 2002; Jiang *et al.*, 2005) show that with the increase of temperature, the glacial area is decreasing. More snow melt runoff caused discharge increases at the three stations in the upper basin, where human activity is less.

Figure 4(a) and (b) shows the change of monthly runoff averaged over a decade in the upstream and downstream of the basin. The grey bar represents an increase range for the past 50 years, and the black bar shows a decrease range. At the upstream station (Xehera), the warmer temperature (Fig. 3(b)) has resulted in a larger increase of runoff in summer, due to more water melted from snow, which is another signal of the influence of climate change on the regional hydrology. It is difficult to see this increasing signal at the downstream Aral station in every month due to the large amount of water withdrawn from the rivers (Zhang *et al.*, 2010). In other words, the hydrological regimes in the headwaters of the Aksu Basin are greatly influenced by climate conditions. However, human activity reduces the amplitude of the trend or causes the change in the opposite direction after the river passes through the city of Akesu, which is the main part of man-made oasis in the basin. This explains how, due to the combined effect of climate and human activity, it is not appropriate to use runoff data to determine WCMMO directly.

Figure 5 displays the MMOI data and their change over time. The MMOI in MMS increased in winter and decreased in summer. Over the NS or WS, the R^2 of the increasing trend is lower or the trend is decreasing. Liu *et al.* (2008) shows that the EMMO of Aksu city increased from 1987 km^2 in 1975 to 2865 km^2 in 2000 and 3608 km^2 in 2005. The winter MMOI in MMS matched this trend well. This indicates again that winter MMOI in MMS is a good index for quantifying the extent of man-made oasis. Assuming the change of EMMO, expressed as Y_a, is linear, with the data provided in Liu *et al.* (2008), we can obtain a linear equation for Y_a as follows:

$$Y_a = 148.6X + 2716.4 \quad (4)$$

where X is the order number of the year. Denoting MMOI in winter in MMS as Y_m, the linear

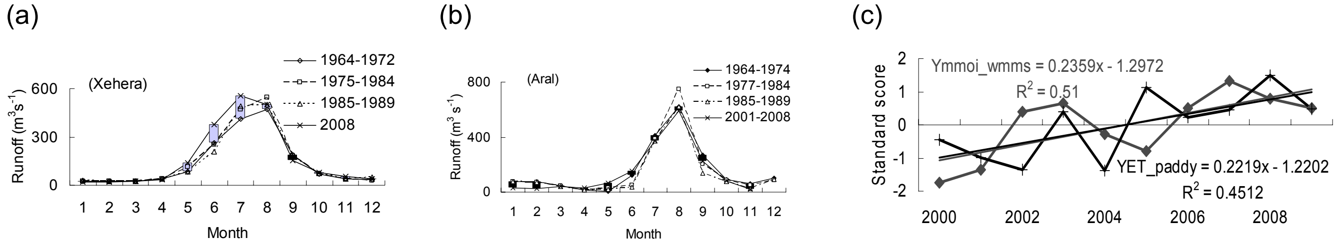

Fig. 4 Comparison of mean monthly runoff at: (a) Xehera, (b) Aral station, and (c) the standard score of ET for paddy field and winter MMO in MMS.

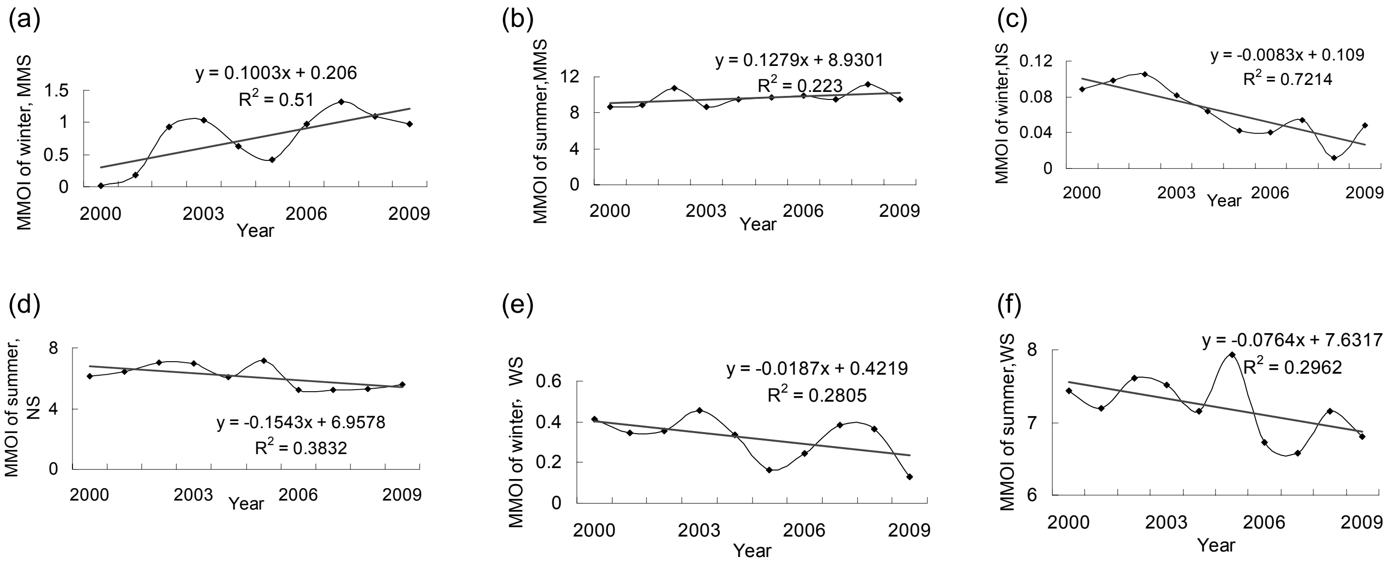

Fig. 5 MMOI in (a) winter, MMS (b) summer, MMS (c) winter, NS (d) summer, NS (e) winter, WS, and (f) summer, WS.

equation from Fig. 5(a) can be written as:

$$Y_m = 0.1003X + 0.206 \quad (5)$$

From the above two linear equations, we obtain the transfer function between Y_m and Y_a as:

$$Y_a = 1482Y_m + 2411 \quad (6)$$

As mentioned in the introduction, it is difficult to calculate the WCMMO from river runoff. We therefore use the VIP model to simulate ET. By combing ET with the information about EMMO as shown in equation (6), we can determine WCMMO.

ET has some advantages over runoff in detecting WCMMO as its spatial pattern is closely related with the land use regimes. However, it is a challenge to validate the modelled ET data. Usually the water balance method is a good tool to validate simulated ET (Mo *et al*., 2004). In our study basin, this is difficult due to the unknown amount of water withdrawal for various activities. Therefore, we cannot use observed runoff to estimate WCMMO. We thus have to compare our results with other studies. Lei *et al*. (2006) estimated ET over the irrigated land as 686 mm/year. Average annual ET simulated by VIP model is 889 mm for the whole basin and 698 mm for the paddy land (Fig. 1(c)). These results matched well with the documented study.

By overlaying the land-use map and 2000 m dividing-line from the DEM, we obtain the land use distribution for NS and MMS. Then the grid numbers of each land use type in NS, WS and MMS are obtained using ArcGIS. We found that paddy field only exists in the MMS. From the distributed results of ET simulated by VIP, we get the ET from paddy field and an increasing trend (Fig. 4(c)). The increases of winter MMO in MMS matched well with the ET trend for paddy field.

By choosing ET for paddy field as the representative rate of WCMMO per unit of EMMO, we then can obtain a clear picture of WCMMO, by multiplying the annual ET rate with Y_m (equation (6)), as shown in Table 2.

Table 2 WCMMO results based on the ET simulated by VIP model and EMMO based on the new index MMOI.

Year	2000	2001	2002	2003	2004	2005	2006	2007
WCMMO (10^8 m^3)	16.58	17.64	24.25	28.12	21.41	22.60	27.34	31.31

CONCLUSIONS

The NDVI spatial data from the MODIS 13 over the Aksu Basin are classified into seven categories based on fractional vegetation cover. The whole study area (WS) is divided into man-made sub-region (MMS) and natural sub-region (NS), with a special consideration of the seasonal, summer–winter difference. A new index, called the man-made oasis index (MMOI) to describe the extent of man-made oasis (EMMO) is developed. It is expressed as the linear weighted combination of the ratio of the area of each class (from III to VI) to the whole area. The special choice of classes III to VI is based on careful observation of the differences among the seven classes in winter and summer. In NS, classes III to VI all disappear in winter, while all classes exist in MMS during 2000 to 2009. MMOI shows an increasing trend. During this period, the man-made oasis was extending greatly (Liu *et al*., 2008). This match encourages us to choose the contribution of classes III to VI as the footprint of man-made oasis. A transfer function between MMOI and EMMO was then derived to calculate the EMMO based on MMOI. As paddy field was found only in MMS, evapotranspiration over the paddy field (ET_p) simulated by the VIP eco-hydrological model was chosen as the representative rate of water consumption by man-made oasis (WCMMO) per unit of EMMO. WCMMO is then calculated annually based on the information of Etp, EMMO and the index MMOI. The results of yearly WCMMO are useful for decision makers to monitor the extent of man-made oasis and make a sustainable plan beneficial to local economical development, the downstream environment, and ecosystem protection.

Acknowledgements This study was jointly supported by the Chinese Ministry of Science and Technology for "973" project (2009CB421300, 2010CB428404), International Cooperation project (0911) and water special key project (2009ZX07210-006), Natural Science Foundation of China grant (41071024, 40830636), the Knowledge Innovation Project of Chinese Academy of Sciences (KZCX2-YW-Q06-1-3). Thanks to the great efforts of the reviewers to help improve this paper.

REFERENCES

Chen, J. *et al*. (2001) Sub- pixel model for vegetation fraction estimation based on land cover classification. *J. Remote Sensing* **5**(6), 416–423 (in Chinese).

Farquhar, G. D., von Caemmerer, S. & Berry, J. A. (1980) A biochemical model of photosynthetic CO_2 assimilation in leaves of C3 species. *Planta* **149**, 78–90.

Lei, Z., Hu, H. & Yang, S. (2006) The analysis of oasis water consumption in Tarim basin. *Shuilixuebao* **37**(2), 1470–1475 (in Chinese).

Liu, J., Gao, M. & Su, J. (2008) Analysis of oasis temporal and spatial variation at northern Tarim Basin based on RS and GIS. *Resources Environment and Development* **2**, 13–16 (in Chinese).

Jiang,Y., Zhou, C. H. & Cheng, W. M (2005) Analysis on runoff supply and variation characteristics of Aksu drainage basin. *J. Natural Resources* **20**(1), 27–34 (in Chinese).

Mo, X., Liu, S., Lin, Z. & Zhao, W. (2004) Simulating temporal and spatial variation of evapotranspiration over the Lushi basin. *J. Hydrol.* **285**, 125–142.

Mo, Xingguo, Liu,Suxia, Lin Zhonghui & Guo Ruiping (2009) Regional crop yield, water consumption and water use efficiency and their responses to climate change in the North China Plain. *Agric. Ecosystems & Environ.* **134**, 67–78.

Shi, Y., F. Sheng, Y. P. & Hu, R. J. (2002) Preliminary study on signal, impact and foreground of climatic shift from warm-dry to warm-humid in Northwest China. *J. Glaciology and Geocryology* **24**(3), 219–226 (in Chinese).

Wang, G. Y. (2008) Runoff changes in Aksu River basin during 1956–2006 and there impacts on water availability for Tarim River. *J. Glaciology and Geocryology* **30**(4), 562–569 (in Chinese).

Zhao, R. J. (1992) The Xinanjiang model applied in China. *J. Hydrol*. **135**, 371–381.

Zhang, S. (2010) Assessing the impact of climate change and human activities on the hydrological processes in the Aksu River Basin. MSc Thesis. Institute of Geographic Sciences and Natural Resources Research. Beijing, China.

Zhang, S. H., Liu, S. X., Mo, X. G., Shu, C., Sun, Y. & Zhang, C. (2011) Assessing the impact of climate change on potential evapotranspiration in the Aksu River Basin. *J. Geogr. Sci*. **21**(3), 1–12.